Electronic Supplementary Material (ESI) for Energy & Environmental Science.

Electronic Supplementary Information

Atomically Inner Tandem Catalysts for Electrochemical Reduction of Carbon Dioxide

Yan Liu,[†*a] Huimei Chen,[†a] Yan Yang,[a] Chi Jiao,[a] Wenkun Zhu,[b] Yaping Zhang,[b] Xiaojun Wu,[c] Junjie Mao[*a] and Zhiwen Zhuo[*a]

[a]Key Laboratory of Functional Molecular Solids, Ministry of Education, College of Chemistry and Materials Science, Anhui Normal University, Wuhu, Anhui 241002, China

[b]State Key Laboratory of Environment-friendly Energy Materials, Southwest University of Science and Technology, Mianyang, Sichuan 621010, China

[c]School of Chemistry and Materials Sciences, University of Science and Technology of China, Hefei, Anhui 230026, China

[*] Email: ly0201@ahnu.edu.cn; maochem@ahnu.edu.cn; zhuozw@ustc.edu.cn

Table of Contents

Computational Details

Spin-polarized DFT, as implemented in the Vienna Ab-initio Simulation Package (VASP) is applied for all calculations.[1,2] The generalized gradient approximation (GGA) with the parametrization of Perdew-Burke-Ernzerhof (PBE) is selected for describing the electron interaction, while the projector augmented wavefunction (PAW) method is utilized to describe the ion-electron interactions.[3,4] A vacuum space of 15 Å is inserted to eliminate the interaction between adjacent periodic units. For all geometry relaxation calculations reported herein, a 500 eV cutoff for the kinetic energy of the plane-wave basis-set and a $3 \times 3 \times 1$ Monkhorst-Pack k-grid is used for sampling the Brillouin zones at structure calculation. The convergence criteria of structure optimization are chosen as the maximum force on each atom less than 0.02 eV/Å with an energy change less than 1×10^{-5} eV.

The Gibbs free energy diagrams for the CO_2RR were used to evaluate the catalytic activity of Co-N-M, according to the Computational Hydrogen Electrode (CHE) model developed by Nørskov *et al.*[5] In the CHE model, the free energy of the electron-proton pair ($H^+ + e^-$) was referenced to the chemical potential of gaseous H_2 at equilibrium (0 V vs Standard Hydrogen Electrode (SHE)), set to that of 1/2 H_2.

The Gibbs free energy (G) of each state was determined by the equation as listed as below:

$$G = E + E_{ZPE} - TS + G_{pH} + G_U$$

Where the E, E_{ZPE}, and S are the electronic energy, the zero-point energy, and the entropy, respectively. T is the reaction temperature. G_{pH} is the free energy correction contributed from pH. G_U is the electrode potential U.

Therefore, the **Gibbs free energy change (ΔG)** of each elementary reaction step was defined as:

$$\Delta G = \Delta E + \Delta E_{ZPE} - T\Delta S + \Delta G_{pH} + \Delta G_U$$

Where the ΔE, ΔE_{ZPE}, and ΔS are the electronic energy difference for the reaction steps, the change of zero-point energy, and the change of entropy, respectively. T is set to room temperature (T = 298.15 K) in this work. ΔG_{pH} is the contribution of the pH ($\Delta G_{pH} = K_BT \times \ln 10 \times pH$, K_B is the Boltzmann constant, pH = 0 in this work). ΔG_U is the free energy contribution related to electrode potential (ΔG_U = -eU, U = 0 V vs SHE in this work). The ZPE and entropies of free molecules (CO_2, CH_4, H_2, H_2O, etc.) at 298.15 K and 1 atm were obtained from the NIST database.[6] Table S1 and S2 present the ZPE and entropy correction for free molecules and adsorbed intermediates on Co-N-M, respectively.

The limiting potential (U_L) was calculated as:

$$U_L = -\Delta G_{PDS}/e$$

Where ΔG_{PDS} is the Gibbs energy change of the potential-determining step (PDS) in CO_2RR, and e is the elementary charge.

The absorption energy (E_{ads}) of an adsorbate $C_xH_yO_z$ ($E_{ads,\ CxHyOz}$) on an adsorbent (*) was applied to estimate the binding strength of an adsorbate $C_xH_yO_z$. Here, all the intermediates of CO_2RR were technically represented by a general chemical formula of $C_xH_yO_z$ (x, y, and z are variables, which were determined according to the real chemical formula of each specific intermediate). The absorption energy (E_{ads}) of the $C_xH_yO_z$ ($E_{ads,\ *CxHyOz}$) was calculated by the equation as listed below:

$$E_{ads,\ *CxHyOz} = E_{*CxHyOz} - E_{*} - E_{CxHyOz}$$

where $E_{*CxHyOz}$, E_*, E_{CxHyOz} represent the electronic energy of the Co-N-M after the intermediate $C_xH_yO_z$ adsorption, the Co-N-M, and the intermediate $C_xH_yO_z$, respectively. According to the definition, a more negative value of $E_{ads,\ *CxHyOz}$ represents a stronger binding strength of $C_xH_yO_z$ in absorption.[7]

The adsorption free energy of $C_xH_yO_z$ ($\Delta G_{*CxHyOz}$) was defined as the equation as listed below:

$$\Delta G_{*CxHyOz} = G_{*CxHyOz} - G_{*} - G_{CxHyOz}$$

where $G_{*CxHyOz}$, G_*, and G_{CxHyOz} represent the Gibbs free energy of the Co-N-M with intermediate $C_xH_yO_z$ adsorption, the Co-N-M, and the intermediate $C_xH_yO_z$, respectively.

The Gibbs free energy of $C_xH_yO_z$ was referenced to the Gibbs free energy of CO_2(g),

H_2(g), and H_2O(g), which was determined by equation as listed as below:

$$G_{C_xH_yO_z} = xG_{CO_2} + (z-2x)G_{H_2O} + (\frac{y}{2} + 2x - z)G_{H_2}$$

The formation energy (E_f) was calculated by:

$$E_f = (E_{Co\text{-}N\text{-}M} - E_{NC} - E_{Co} - E_M)/2$$

E_{NC} is the electronic energy of the NC framework without central metal atoms. $E_{Co\text{-}N\text{-}M}$ is the electronic energy of Co-N-M catalyst, and M represents different metals.

The dissolution potential (U_{diss}) calculated in this work was according to the theory model proposed by J. K. Nørskov, *et al.*,[8] and the calculated equations of dissolution potential of Co atom ($U_{diss,\ Co}$ (vs. SHE)) and M atom ($U_{diss,\ M}$ (vs. SHE)) in the Co-N-M system were listed as below:

$$U_{diss,\ Co} = U^0_{diss(Co,\ bulk)} - (E_{Co\text{-}N\text{-}M} - E_{M\text{-}NC} - E_{Co,\ bulk})/n_{Co}e, \text{ (pH=0)}$$

$$U_{diss,\ M} = U^0_{diss(M,\ bulk)} - (E_{Co\text{-}N\text{-}M} - E_{Co\text{-}NC} - E_{M,\ bulk})/n_{M}e, \text{ (pH=0)}$$

where the $U^0_{diss(Co,\ bulk)}$ and $U^0_{diss(M,\ bulk)}$ are the standard dissolution potential of Co and M bulk metals at pH = 0; $E_{Co\text{-}N\text{-}M}$ is the electronic energy of Co-N-M structure; $E_{M\text{-}NC}$ and $E_{Co\text{-}NC}$ are the electronic energy of Co-N-M structure without Co atom and that without M atom; $E_{Co,\ bulk}$ and $E_{M,bulk}$ are the single atom electronic energy of Co atom in Co bulk metal, and that of M atom in M bulk metal; n_{Co} and n_M are the transfer electron number of Co atom and M atom in the dissolution process, respectively. The standard dissolution potential (U^0_{diss}) of each metal atom was taken from the previous work,[9] as listed in Table S3, and the dissolution potential of selected metal atoms in the Co-N-M system were listed in Table S4.

Ab initio molecular dynamics (AIMD) simulations in constant temperature and volume with a Nose–Hoover thermostat[10] were adopted to evaluate the thermodynamic stability of the Co-N-M, and the stability of the optimal catalyst Co-N-Cr under realistic conditions, including electric field, explicit water molecules, and possible reaction fragments, such as OH, H, and CO_3 exist in the CO_2RR process was simulated. According to the electrical double layer model[11,12] in electrochemical reaction, the overpotential is the U between the positive charge layer and the negative charge layer, of which the interlayer distance can be as short as the distance between two layers of atoms, about 3-4 Å. Therefore, the vertical electric filed along z-direction with an electric field intensity of 0.1V/Å was applied in the AIMD for the simulation on Co-N-Cr (U_L = -0.35 V).

The crystal orbital Hamilton population (COHP) of metal-adsorbate interactions was used to analyze chemical bonds.[13,14] The analysis was conducted using LOBSTER software.[15] The climb-image nudged elastic band (CI-NEB)[16,17] method was employed to search for the minimum energy pathways. The relevant structure files are available in the ioChem-BD repository (https://www.iochem-bd.org/).

Elementary steps of CO_2RR pathway from CO_2 to C1 products

Formation of CO:

The overall formula of formation of CO:

$$* + CO_2 + 2H^+ + 2e^- \rightarrow CO + H_2O$$

which is divided into:

$$* + CO_2 + H^+ + e^- \rightarrow *COOH$$

$$*COOH + H^+ + e^- \rightarrow *CO + H_2O$$

$$*CO \rightarrow * + CO$$

Formation of HCOOH:

The overall formula of formation of HCOOH:

$$* + CO_2 + 2H^+ + 2e^- \rightarrow HCOOH$$

which is divided into:

$$* + CO_2 + H^+ + e^- \rightarrow *HCOO$$

$$*HCOO + H^+ + e^- \rightarrow *HCOOH$$

$$*HCOOH \rightarrow * + HCOOH$$

Formation of CH_3OH:

The overall formula of formation of CH_3OH:

$$CO_2 + 6H^+ + 2e^- \rightarrow CH_3OH + H_2O$$

which is divided into:

Path 1:

$$* + CO_2 + H^+ + e^- \rightarrow *COOH$$

$$*COOH + H^+ + e^- \rightarrow *CO + H_2O$$

$$*CO + H^+ + e^- \rightarrow *COH$$

$$*COH + H^+ + e^- \rightarrow *CHOH$$

$$*CHOH + H^+ + e^- \rightarrow *CH_2OH$$

$$*CH_2OH + H^+ + e^- \rightarrow *CH_3OH$$

$$*CH_3OH \rightarrow * + CH_3OH$$

Path 2

$$* + CO_2 + H^+ + e^- \rightarrow *COOH$$

$$*COOH + H^+ + e^- \rightarrow *CO + H_2O$$

$$*CO + H^+ + e^- \rightarrow *CHO$$

$$*CHO + H^+ + e^- \rightarrow *CHOH$$

$$*CHOH + H^+ + e^- \rightarrow *CH_2OH$$

$$*CH_2OH + H^+ + e^- \rightarrow *CH_3OH$$

$$*CH_3OH \rightarrow * + CH_3OH$$

Path 3:

$$* + CO_2 + H^+ + e^- \rightarrow *HCOO$$

$$*HCOO + H^+ + e^- \rightarrow *HCOOH$$

$$*HCOOH + H^+ + e^- \rightarrow *CHO + H_2O$$

$$*CHO + H^+ + e^- \rightarrow *CHOH$$

$$*CHOH + H^+ + e^- \rightarrow *CH_2OH$$

$$*CH_2OH + H^+ + e^- \rightarrow *CH_3OH$$

$$*CH_3OH \rightarrow * + CH_3OH$$

Path 4:

$$* + CO_2 + H^+ + e^- \rightarrow *HCOO$$

$$*HCOO + H^+ + e^- \rightarrow *HCOOH$$

$$*HCOOH + H^+ + e^- \rightarrow *CHO + H_2O$$

$$*CHO + H^+ + e^- \rightarrow *OCH_2$$

$$*OCH_2 + H^+ + e^- \rightarrow *OCH_3$$

$$*OCH_3 + H^+ + e^- \rightarrow *CH_3OH$$

$$*CH_3OH \rightarrow * + CH_3OH$$

Formation of CH_4:

The overall formula of formation of CH_4:

$$CO_2 + 8H^+ + 2e^- \rightarrow CH_4 + 2H_2O$$

which is divided into:

Path 1:

$$* + CO_2 + H^+ + e^- \rightarrow *COOH$$

$$*COOH + H^+ + e^- \rightarrow *CO + H_2O$$

$$*CO + H^+ + e^- \rightarrow *COH$$

$$*COH + H^+ + e^- \rightarrow *CHOH$$

$$*CHOH + H^+ + e^- \rightarrow *CH + *H_2O$$

$$*CH + H^+ + e^- \rightarrow *CH_2$$

$$*CH_2 + H^+ + e^- \rightarrow *CH_3$$

$$*CH_3 + H^+ + e^- \rightarrow *+ CH_4$$

Path 2:

$$* + CO_2 + H^+ + e^- \rightarrow *COOH$$

$$*COOH + H^+ + e^- \rightarrow *CO + H_2O$$

$$*CO + H^+ + e^- \rightarrow *CHO$$

$$*CHO + H^+ + e^- \rightarrow *CHOH$$

$$*CHOH + H^+ + e^- \rightarrow *CH + *H_2O$$

$$*CH + H^+ + e^- \rightarrow *CH_2$$

$$*CH_2 + H^+ + e^- \rightarrow *CH_3$$

$$*CH_3 + H^+ + e^- \rightarrow * + CH_4$$

Path 3:

$$*+CO_2 + H^+ + e^- \rightarrow *COOH$$

$$*COOH + H^+ + e^- \rightarrow *CO + H_2O$$

$$*CO + H^+ + e^- \rightarrow *CHO$$

$$*CHO + H^+ + e^- \rightarrow *OCH_2$$

$$*OCH_2 + H^+ + e^- \rightarrow *OCH_3$$

$$*OCH_3 + H^+ + e^- \rightarrow *O + CH_4$$

$$*O+ H^+ + e^- \rightarrow *OH$$

$$*OH + H^+ + e^- \rightarrow *+ H_2O$$

Path 4:

$$* + CO_2 + H^+ + e^- \rightarrow *HCOO$$

$$*HCOO + H^+ + e^- \rightarrow *HCOOH$$

$$*HCOOH + H^+ + e^- \rightarrow *CHO + H_2O$$

$$*CHO + H^+ + e^- \rightarrow *CHOH$$

$$*CHOH + H^+ + e^- \rightarrow *CH + *H_2O$$

$$*CH + H^+ + e^- \rightarrow *CH_2$$

$$*CH_2 + H^+ + e^- \rightarrow *CH_3$$

$$*CH_3 + H^+ + e^- \rightarrow * + CH_4$$

Path 5:

$$* + CO_2 + H^+ + e^- \rightarrow *HCOO$$

$$*HCOO + H^+ + e^- \rightarrow *HCOOH$$

$$*HCOOH + H^+ + e^- \rightarrow *CHO + H_2O$$

$$*CHO + H^+ + e^- \rightarrow *OCH_2$$

$$*OCH_2 + H^+ + e^- \rightarrow *OCH_3$$

$$*OCH_3 + H^+ + e^- \rightarrow *O + CH_4$$

$$*O+ H^+ + e^- \rightarrow *OH$$

$$*OH + H^+ + e^- \rightarrow *+ H_2O$$

Table S1 The computed zero-point energies (ZPE) and entropies multiplied by T (T = 298.15 K) (-TS) for gas phase molecules

Gas molecule	ZPE (eV)	-TS (eV)
CO	0.13	-0.62
CO_2	0.31	-0.67
H_2	0.27	-0.40
H_2O	0.57	-0.67
HCOOH	0.88	-0.78
CH_3OH	1.34	-0.75
CH_4	1.17	-0.58

Table S2 The computed zero-point energies (ZPE) and entropies multiplied by T (T = 298.15 K) (-TS) for adsorbed species

Adsorbed species	ZPE (eV)	-TS (eV)
*COOH	0.64	-0.19
*HCOO	0.62	-0.18
*CO	0.21	-0.13
*CHO	0.48	-0.13
*COH	0.44	-0.16
[a]$*OCH_2$	0.70	-0.20
[b]$*OCH_2$	0.84	-0.16
*CHOH	0.80	-0.15
$*OCH_3$	1.09	-0.20
*O	0.08	-0.05
*OH	0.33	-0.15
*CH	0.31	-0.09
$*CH_2$	0.59	-0.14
$*CH_3$	0.96	-0.15

a: Only the O atom in $*OCH_2$ binds to M site.

b: The O and C atoms in $*OCH_2$ bind to M and N site, respectively.

Table S3 The standard dissolution potentials (U^0_{diss}) (pH = 0) for the pure metals, and the number of transferred electrons (n_e) of corresponding metal atom during the dissolution

Metel	**U^0_{diss} (V)**	**n_e**
Cr	-0.91	2
Mn	-1.19	2
Fe	-0.45	2
Co	-0.28	2
Ni	-0.26	2
Cu	0.34	2

Table S4 The dissolution potential (U_{diss}) (pH = 0) of each metal atom in the Co-N-M system

Metel	**U_{diss} (V)**
Co_1N_4	0.91
Co-N-Cr_Co	0.82
Co-N-Cr_Cr	0.54
Co-N-Mn_Co	0.83
Co-N-Mn_Mn	0.43
Co-N-Fe_Co	0.81
Co-N-Fe_Fe	0.64
Co-N-Co_Co	0.94
Co-N-Ni_Co	0.93
Co-N-Ni_Ni	1.11
Co-N-Cu_Co	0.86
Co-N-Cu_Cu	1.23

The adsorption of CO_2 on Co_1N_4

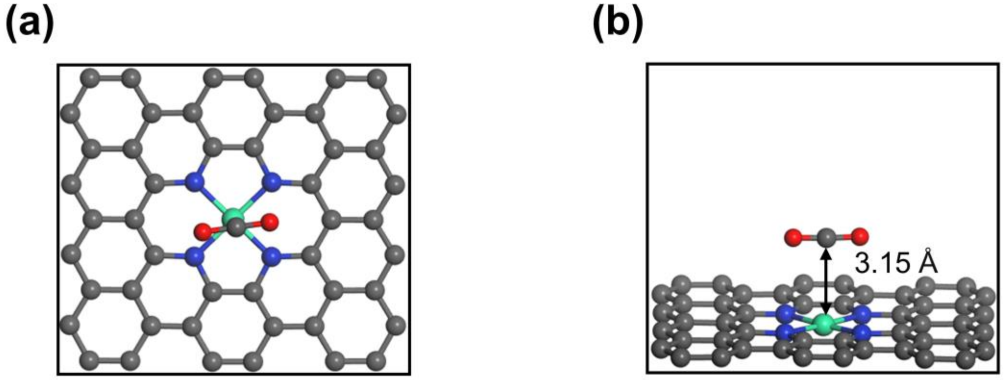

Fig. S1 (a) Top and (b) side views of CO_2 adsorbed on Co_1N_4.

Reaction steps and ΔG of CO_2RR on Co_1N_4

Table S5: Reaction steps and Gibbs free energy changes (ΔG, eV) of CO_2RR to C1 production on Co_1N_4 at room temperature under 1 atm

Reaction steps	ΔG (eV)
$* + CO_2 + H^+ + e^- \rightarrow *COOH$	0.34
$* + CO_2 + H^+ + e^- \rightarrow *HCOO$	0.63
$*HCOO + H^+ + e^- \rightarrow *HCOOH$	-0.03
$*HCOOH \rightarrow * + HCOOH$	-0.43
$*COOH + H^+ + e^- \rightarrow *CO + H_2O$	-0.15
$*CO \rightarrow * + CO$	0.44
$*CO + H^+ + e^- \rightarrow *CHO$	-0.09
$*CO + H^+ + e^- \rightarrow *COH$	1.83
$*CHO + H^+ + e^- \rightarrow *OCH_2$	0.81
$*CHO + H^+ + e^- \rightarrow *CHOH$	1.33
$*OCH_2 + H^+ + e^- \rightarrow *OCH_3$	-0.26
$*OCH_3 + H^+ + e^- \rightarrow *CH_3OH$	-0.43
$*CH_3OH \rightarrow * + CH_3OH$	-0.23
$*OCH_3 + H^+ + e^- \rightarrow *O + CH_4$	0.69
$*O + H^+ + e^- \rightarrow *OH$	-1.68
$*OH + H^+ + e^- \rightarrow * + H_2O$	-0.84

The infrastructure analysis of Co-N-M

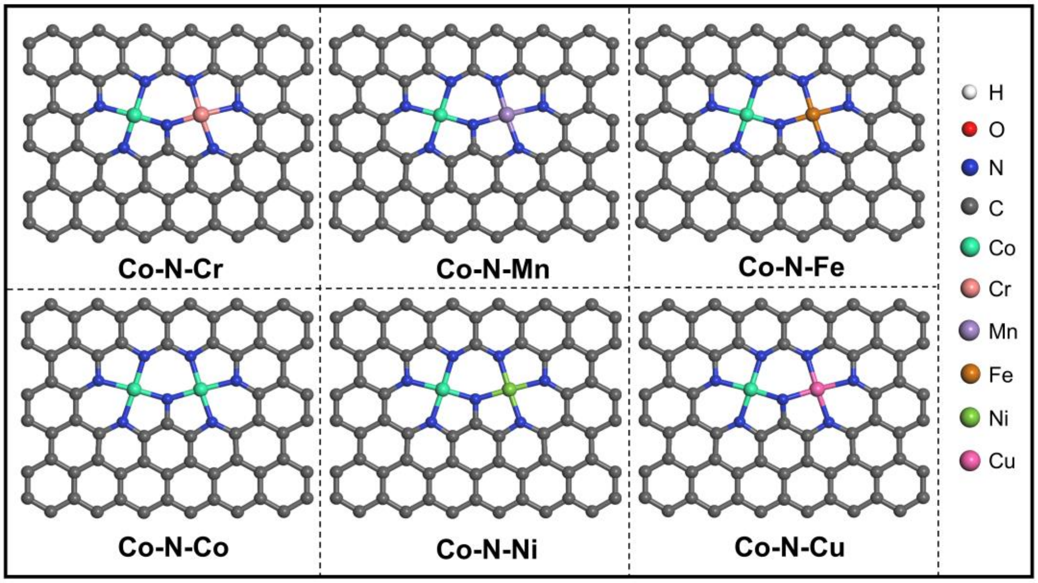

Fig. S2 Optimized structure of the Co-N-M.

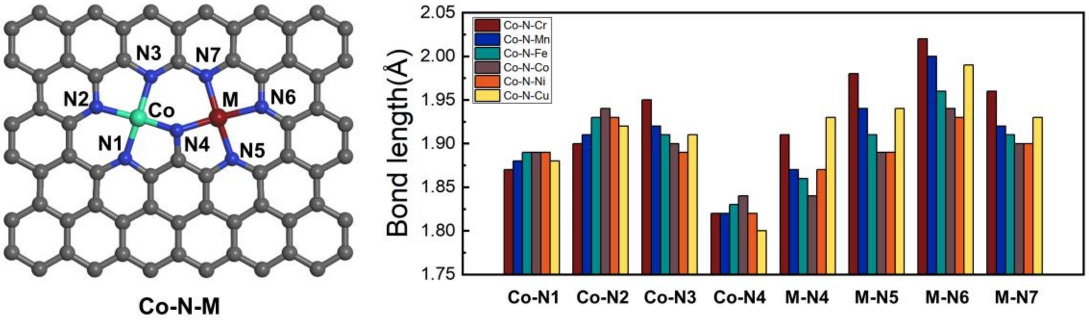

Fig. S3 Bond lengths of M−N in Co-N-M.

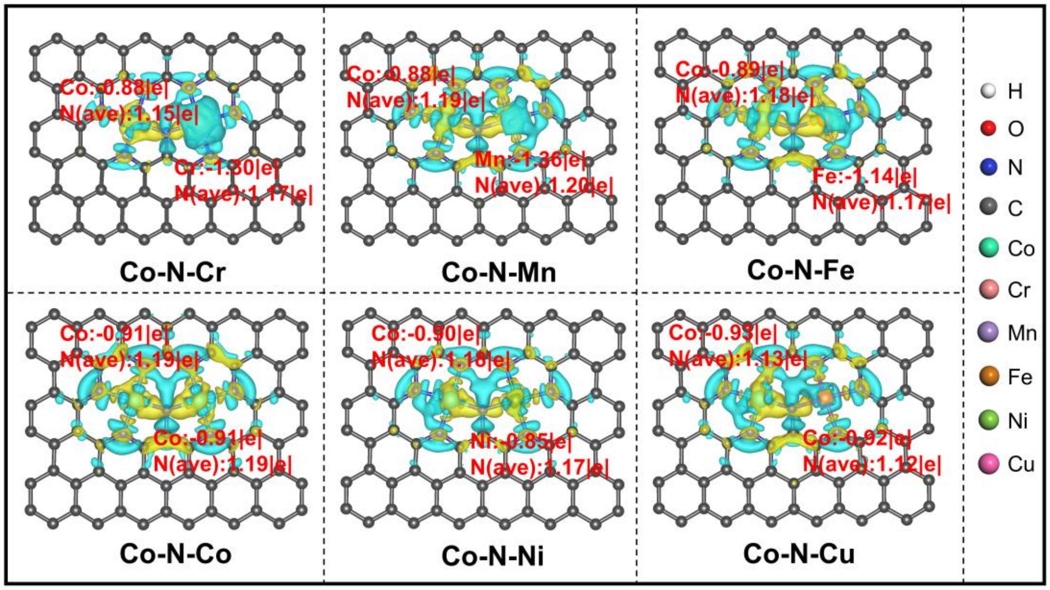

Fig. S4 Charge density difference corresponding with Bader charge analysis of Co-N-M before and after metal atom anchored into framework. The isosurface values were 2×10^{-3} e/$Å^3$. Yellow and cyan regions represent increasing and decreasing electron densities, respectively.

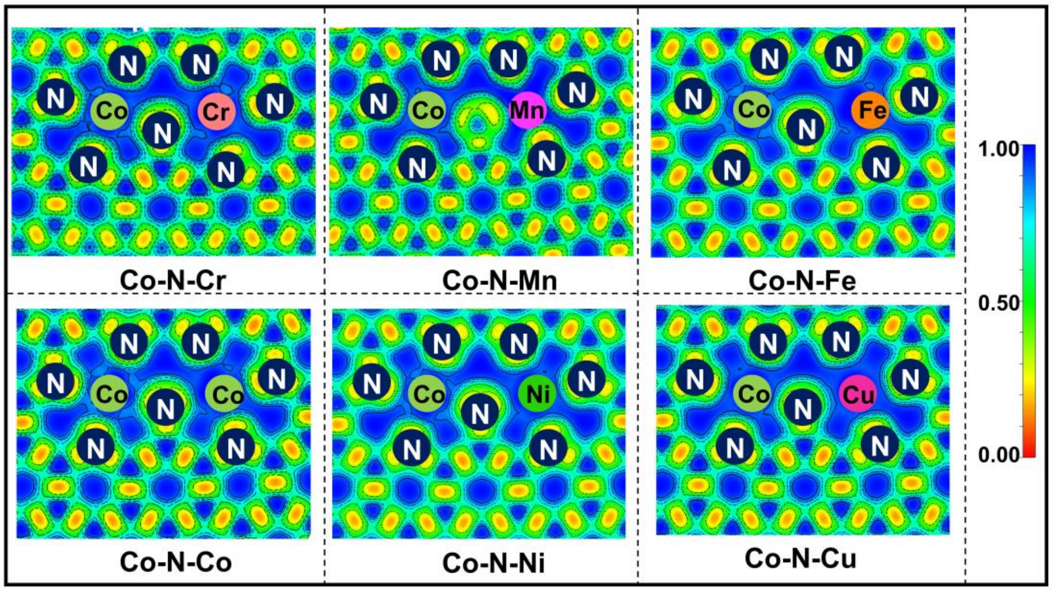

Fig. S5 The electron localization functions (ELF) of Co-N-M.

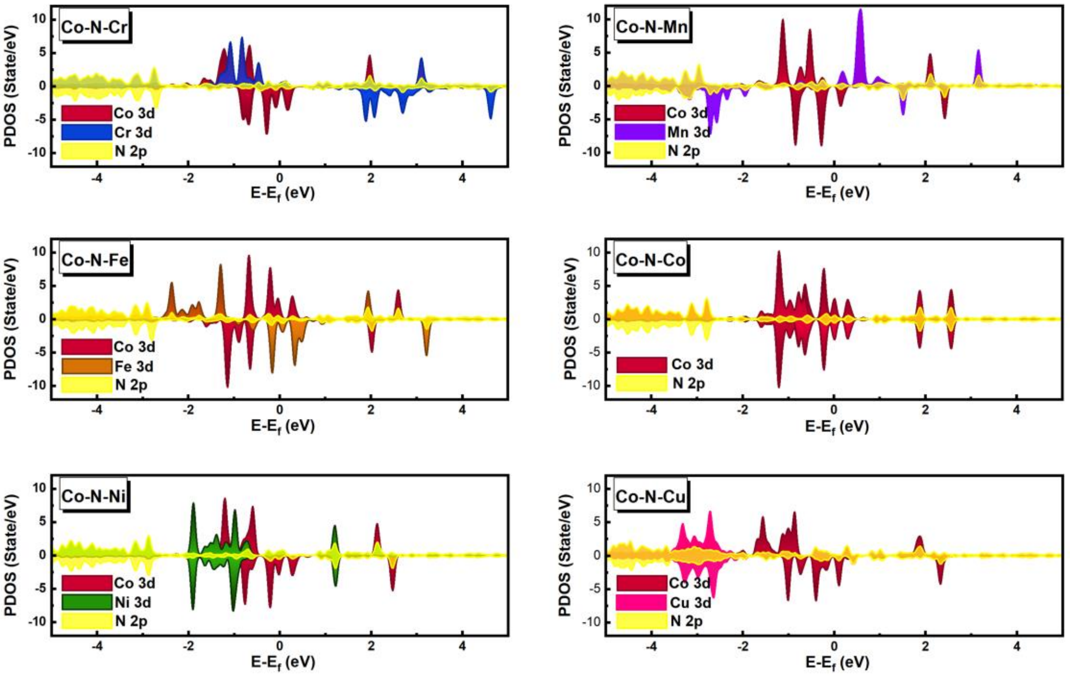

Fig. S6 The projected density of states (PDOS) for 3d orbitals of metals (Co/M), and 2p orbitals of N atoms.

The stability of Co-N-M

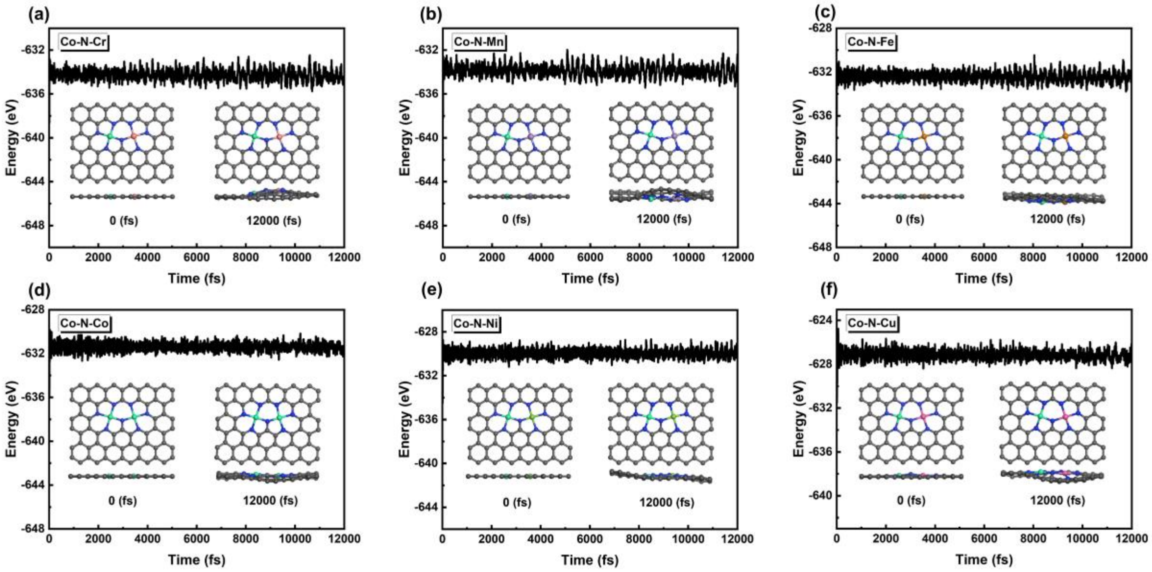

Fig. S7 Energy fluctuations of Co-N-M with time progress of AIMD simulations at 500 K.

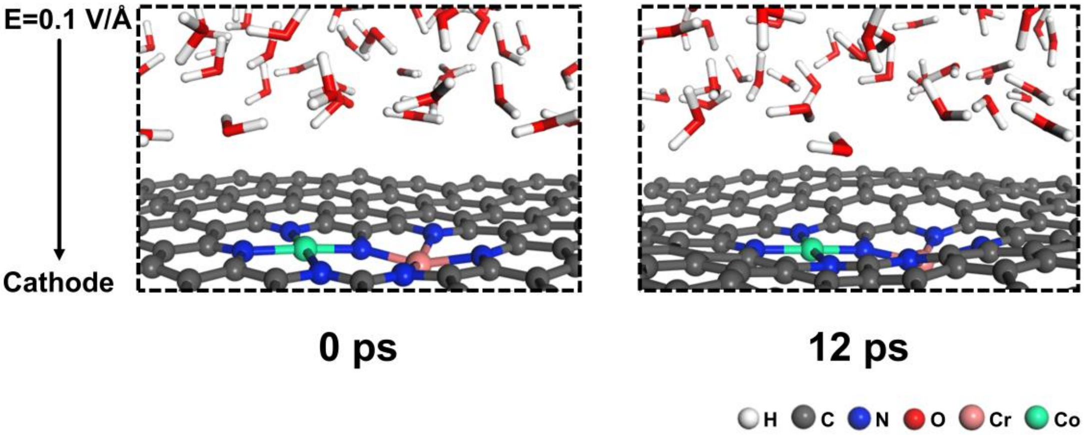

Fig. S8 The AIMD simulation of the stability of Co-N-Cr with the presence of electric field along z-direction and water. The simulation temperature is 300 K with a total time of 12 ps and a time step of 1 fs.

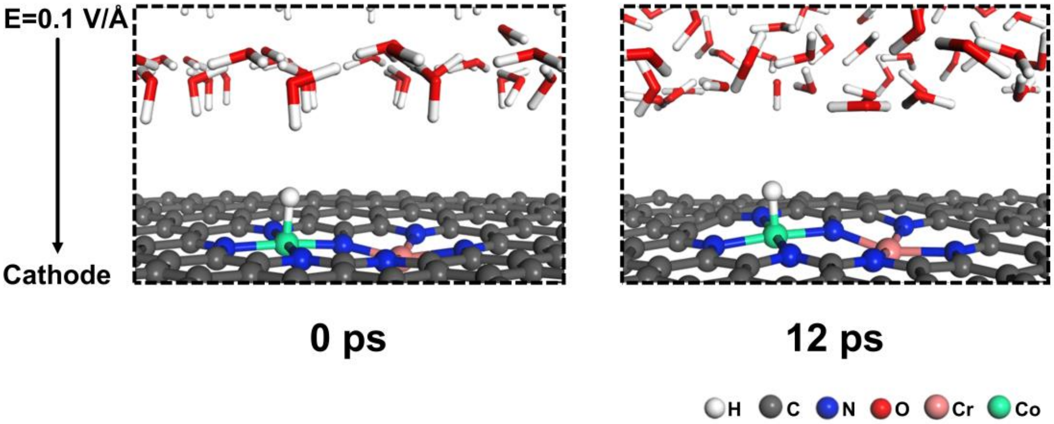

Fig. S9 The AIMD simulation of the stability of Co-N-Cr with the presence of electric field along z-direction, water and reaction fragment H. The simulation temperature is 300 K with a total time of 12 ps and a time step of 1 fs.

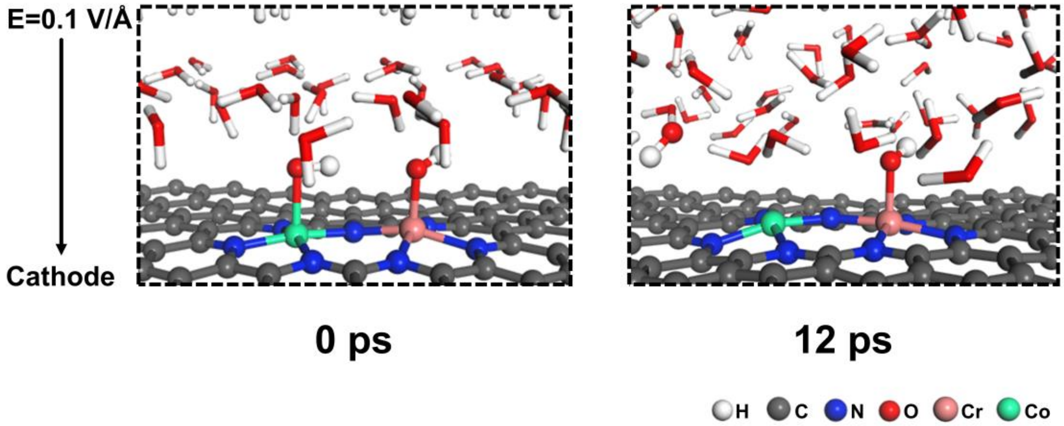

Fig. S10 The AIMD simulation of the stability of Co-N-Cr with the presence of electric field, water and reaction fragment OH. The simulation temperature is 300 K with a total time of 12 ps and a time step of 1 fs.

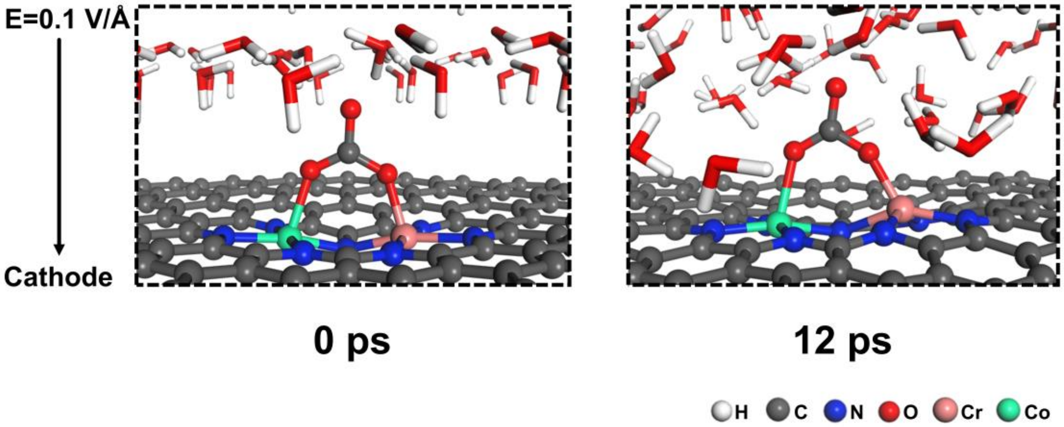

Fig. S11 The AIMD simulation of the stability of Co-N-Cr with the presence of electric field, water and reaction fragment CO_3. The simulation temperature is 300 K with a total time of 12 ps and a time step of 1 fs.

Free energy diagrams of Co-N-M (M=Mn, Fe, Co, Ni, Cu)

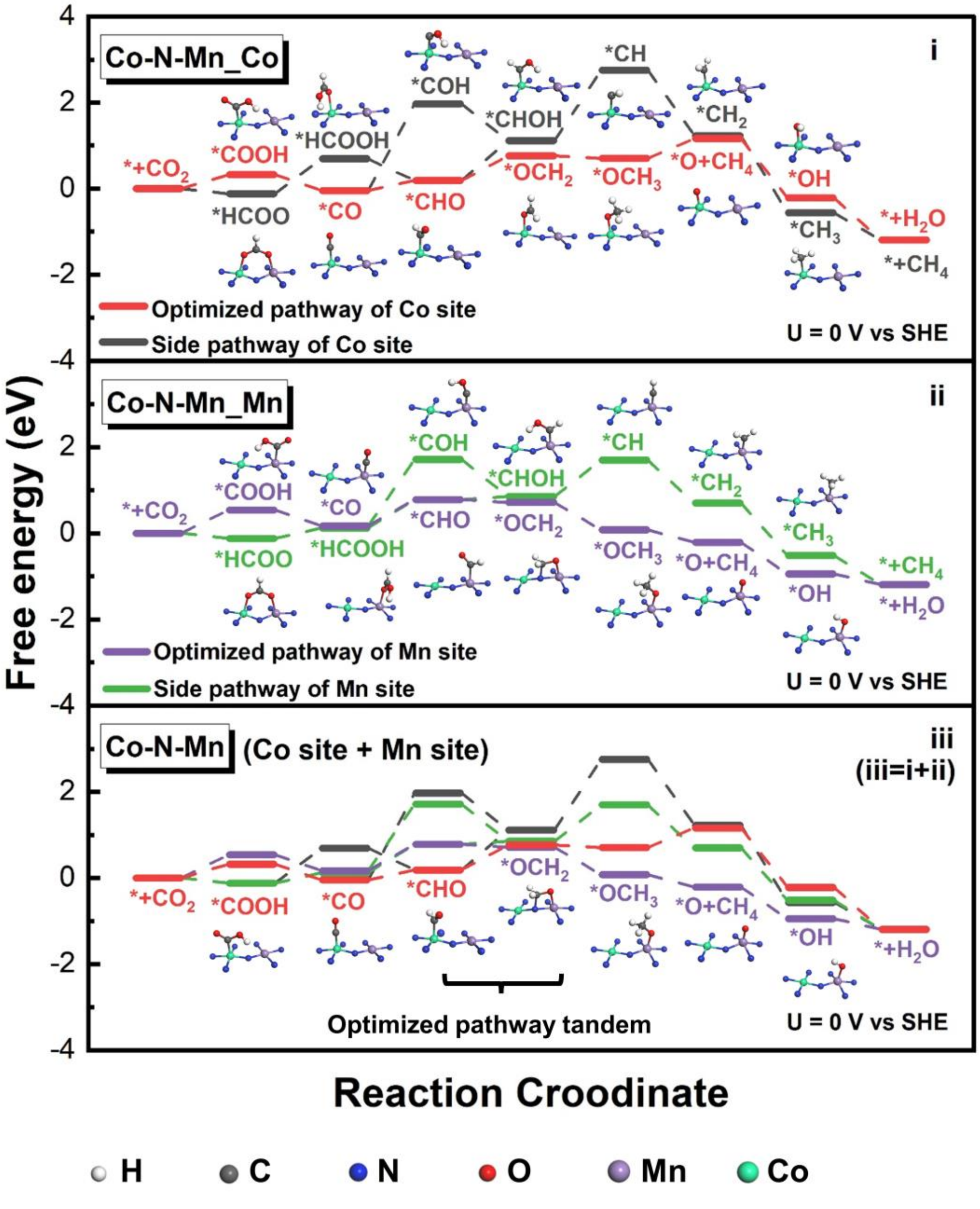

Fig. S12 Free energy diagrams and geometrical structures of CO_2 reduction to CH_4 on Co site (i), Mn site (ii) and the inner tandem combinatorial pathway (iii) of Co-N-Mn.

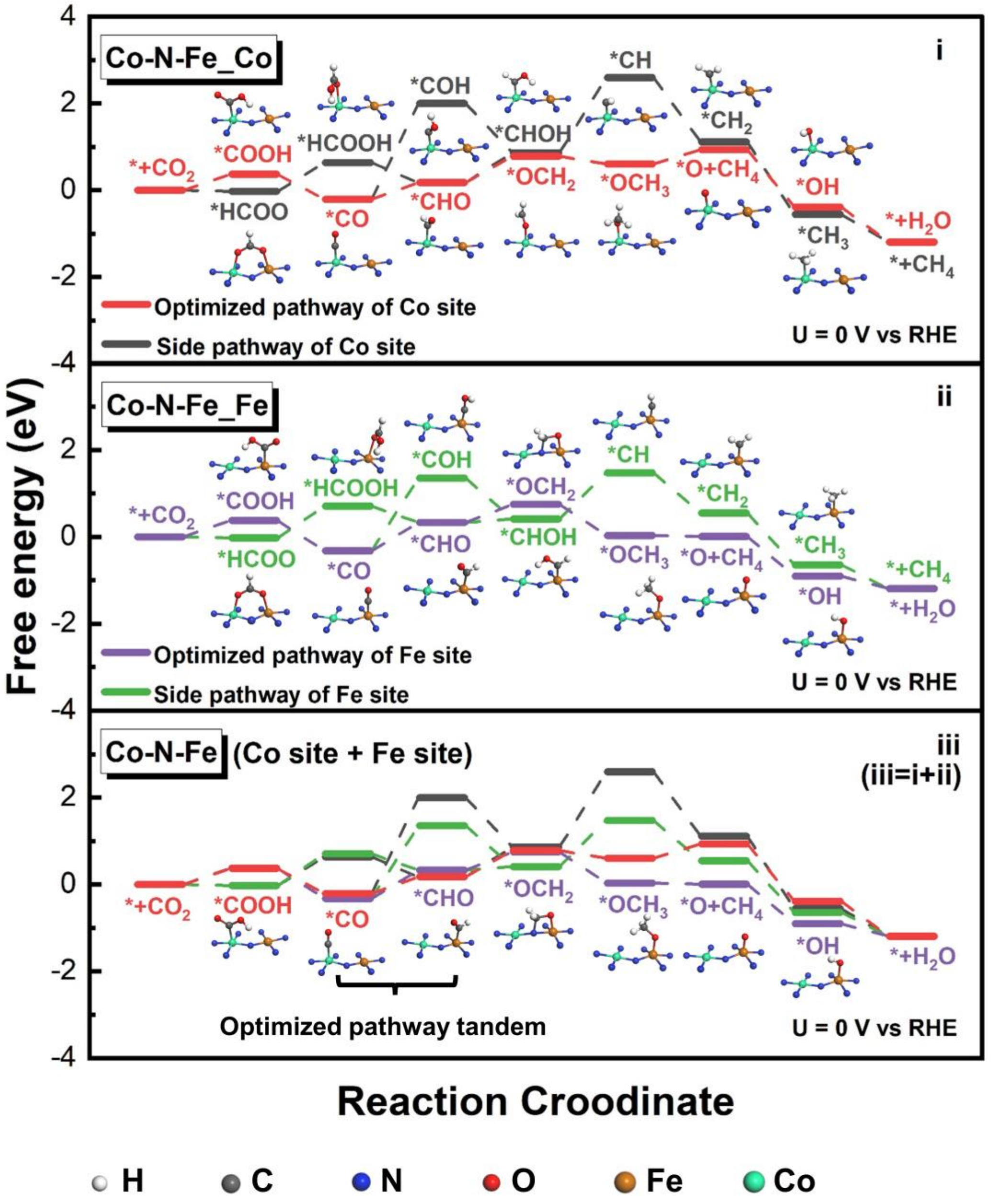

Fig. S13 Free energy diagrams and geometrical structures of CO_2 reduction to CH_4 on Co site (i), Fe site (ii) and the inner tandem combinatorial pathway (iii) of Co-N-Fe.

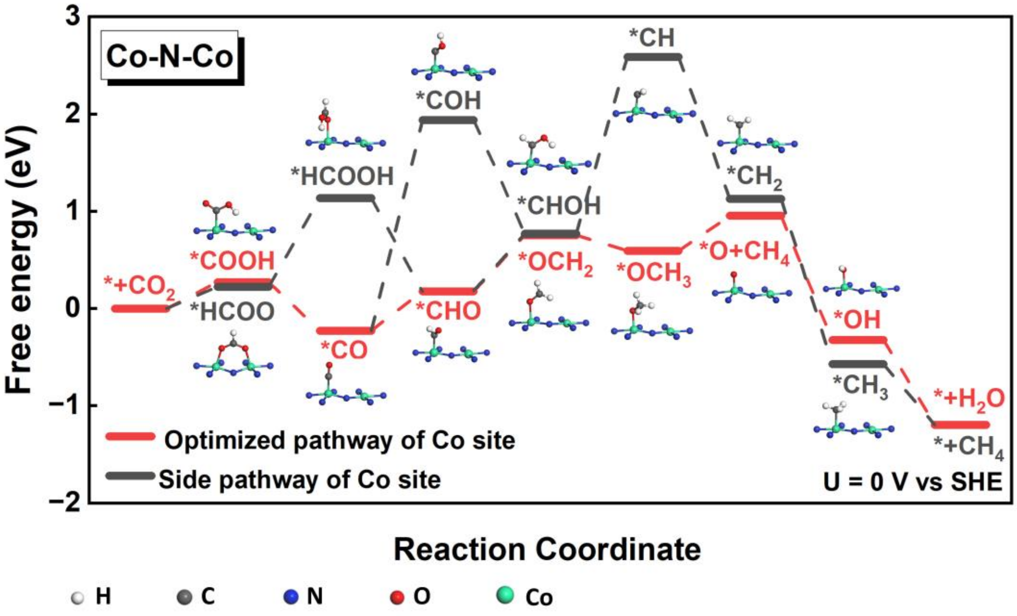

Fig. S14 Free energy diagram and geometrical structures of CO_2 reduction to CH_4 on Co site of Co-N-Co.

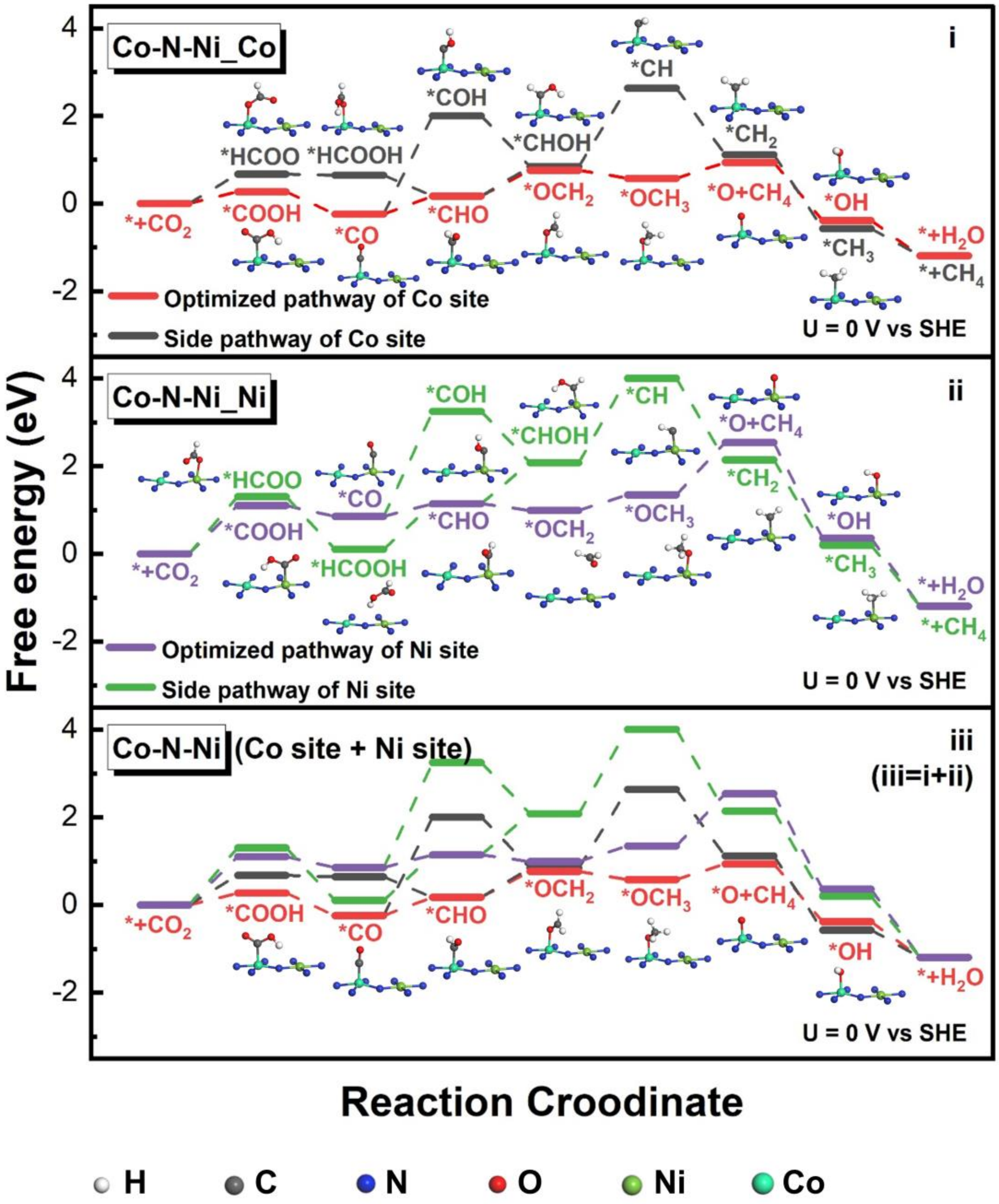

Fig. S15 Free energy diagrams and geometrical structures of CO$_2$ reduction to CH$_4$ on Co site (i), Ni site (ii) and the combinatorial pathway (iii) of Co-N-Ni.

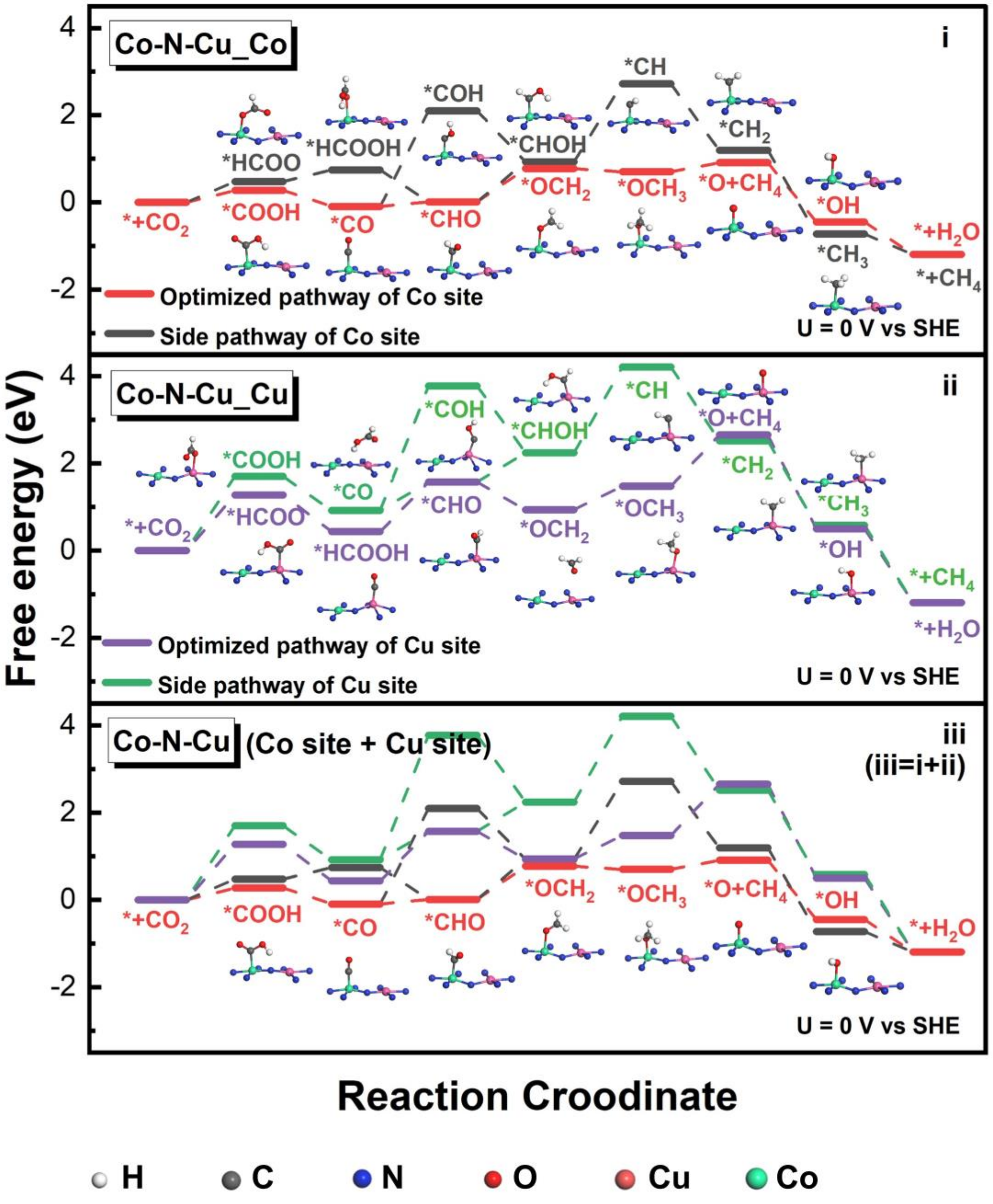

Fig. S16 Free energy diagrams and geometrical structures of CO_2 reduction to CH_4 on Co site (i), Cu site (ii) and the combinatorial pathway (iii) of Co-N-Cu.

Reaction steps and ΔG of CO_2RR on Co-N-M

Table S6: Reaction steps and Gibbs free energy changes (ΔG, eV) of CO_2RR to CH_4 on Co-N-Cr at room temperature under 1 atm

Reaction steps	**ΔG (eV)**		
	Co site	Cr site	Tandem sites
$* + CO_2 + H^+ + e^- \rightarrow *COOH$	0.31	0.44	0.31
$*COOH + H^+ + e^- \rightarrow *CO + H_2O$	-0.52	-0.36	-0.52
$*CO + H^+ + e^- \rightarrow *CHO$	0.35	0.60	0.35
$*CHO + H^+ + e^- \rightarrow *OCH_2$	0.63	-0.60	-0.06
$*OCH_2 + H^+ + e^- \rightarrow *OCH_3$	-0.13	-0.55	-0.55
$*OCH_3 + H^+ + e^- \rightarrow *O + CH_4$	0.28	-0.84	-0.84
$*O + H^+ + e^- \rightarrow *OH$	-1.30	-0.19	-0.19
$*OH + H^+ + e^- \rightarrow * + H_2O$	-0.80	0.30	0.30
$*CHO + H^+ + e^- \rightarrow *CHOH$	0.74	0.01	/
$*CHOH + H^+ + e^- \rightarrow *CH + H_2O$	1.77	0.49	/
$*CH + H^+ + e^- \rightarrow *CH_2$	-1.61	-0.86	/
$*CH_2 + H^+ + e^- \rightarrow *CH_3$	-1.67	-0.98	/
$*CH_3 + H^+ + e^- \rightarrow *+CH_4$	-0.56	-0.53	/
$*CO + H^+ + e^- \rightarrow *COH$	1.88	1.35	/
$*COH + H^+ + e^- \rightarrow *CHOH$	-0.78	-0.74	/
$* + CO_2 + H^+ + e^- \rightarrow *HCOO$	-0.35	-0.35	/
$*HCOO + H^+ + e^- \rightarrow *HCOOH$	0.91	0.29	/
$*HCOOH + H^+ + e^- \rightarrow *CHO + H_2O$	-0.42	0.73	/

Table S7: Reaction steps and Gibbs free energy changes (ΔG, eV) of CO_2RR to CH_4 on Co-N-Mn at room temperature under 1 atm

Reaction steps	**ΔG (eV)**		
	Co site	Mn site	Tandem sites
$* + CO_2 + H^+ + e^- \rightarrow *COOH$	0.32	0.54	0.32
$*COOH + H^+ + e^- \rightarrow *CO + H_2O$	-0.37	-0.37	-0.37
$*CO + H^+ + e^- \rightarrow *CHO$	0.23	0.61	0.23
$*CHO + H^+ + e^- \rightarrow *OCH_2$	0.58	-0.07	0.53
$*OCH_2 + H^+ + e^- \rightarrow *OCH_3$	-0.05	-0.63	-0.63
$*OCH_3 + H^+ + e^- \rightarrow *O + CH_4$	0.46	-0.29	-0.29
$*O + H^+ + e^- \rightarrow *OH$	-1.38	-0.73	-0.73
$*OH + H^+ + e^- \rightarrow * + H_2O$	-0.98	-0.24	-0.24
$*CHO + H^+ + e^- \rightarrow *CHOH$	0.93	0.07	/
$*CHOH + H^+ + e^- \rightarrow *CH + H_2O$	1.64	0.85	/
$*CH + H^+ + e^- \rightarrow *CH_2$	-1.53	-1.00	/
$*CH_2 + H^+ + e^- \rightarrow *CH_3$	-1.79	-1.22	/
$*CH_3 + H^+ + e^- \rightarrow *+CH_4$	-0.63	-0.67	/
$*CO + H^+ + e^- \rightarrow *COH$	2.02	1.54	/
$*COH + H^+ + e^- \rightarrow *CHOH$	-0.86	-0.86	/
$* + CO_2 + H^+ + e^- \rightarrow *HCOO$	-0.12	-0.12	/
$*HCOO + H^+ + e^- \rightarrow *HCOOH$	0.81	0.24	/
$*HCOOH + H^+ + e^- \rightarrow *CHO + H_2O$	-0.51	0.66	/

Table S8: Reaction steps and Gibbs free energy changes (ΔG, eV) of CO_2RR to CH_4 on Co-N-Fe at room temperature under 1 atm

Reaction steps	**ΔG (eV)**			
	Co site	Fe site	[a]Tandem sites	[b]Tandem sites
$* + CO_2 + H^+ + e^- \rightarrow *COOH$	0.37	0.38	0.37	0.37
$*COOH + H^+ + e^- \rightarrow *CO + H_2O$	-0.58	-0.70	-0.58	-0.58
$*CO + H^+ + e^- \rightarrow *CHO$	0.38	0.66	0.54	0.38
$*CHO + H^+ + e^- \rightarrow *OCH_2$	0.61	0.42	0.42	0.57
$*OCH_2 + H^+ + e^- \rightarrow *OCH_3$	-0.18	-0.71	-0.71	-0.71
$*OCH_3 + H^+ + e^- \rightarrow *O + CH_4$	0.33	-0.02	-0.02	-0.02
$*O + H^+ + e^- \rightarrow *OH$	-1.32	-0.91	-0.91	-0.91
$*OH + H^+ + e^- \rightarrow * + H_2O$	-0.81	-0.29	-0.29	-0.29
$*CHO + H^+ + e^- \rightarrow *CHOH$	0.69	0.08	/	/
$*CHOH + H^+ + e^- \rightarrow *CH + H_2O$	1.73	1.06	/	/
$*CH + H^+ + e^- \rightarrow *CH_2$	-1.48	-0.93	/	/
$*CH_2 + H^+ + e^- \rightarrow *CH_3$	-1.67	-1.19	/	/
$*CH_3 + H^+ + e^- \rightarrow *+CH_4$	-0.63	-0.55	/	/
$*CO + H^+ + e^- \rightarrow *COH$	2.21	1.68	/	/
$*COH + H^+ + e^- \rightarrow *CHOH$	-1.13	-0.94	/	/
$* + CO_2 + H^+ + e^- \rightarrow *HCOO$	-0.03	-0.03	/	/
$*HCOO + H^+ + e^- \rightarrow *HCOOH$	0.66	0.74	/	/
$*HCOOH + H^+ + e^- \rightarrow *CHO + H_2O$	-0.46	-0.38	/	/

[a] The tandem process via the Co-*CO to Fe-*CHO.

[b] The tandem process via the Co-*CHO to Fe-*OCH_2.

Table S9: Reaction steps and Gibbs free energy changes (ΔG, eV) of CO_2RR to CH_4 on Co-N-Co at room temperature under 1 atm

Reaction steps	**ΔG (eV)**
$* + CO_2 + H^+ + e^- \rightarrow *COOH$	0.27
$*COOH + H^+ + e^- \rightarrow *CO + H_2O$	-0.50
$*CO + H^+ + e^- \rightarrow *CHO$	0.40
$*CHO + H^+ + e^- \rightarrow *OCH_2$	0.58
$*OCH_2 + H^+ + e^- \rightarrow *OCH_3$	-0.15
$*OCH_3 + H^+ + e^- \rightarrow *O + CH_4$	0.36
$*O + H^+ + e^- \rightarrow *OH$	-1.28
$*OH + H^+ + e^- \rightarrow * + H_2O$	-0.87
$*CHO + H^+ + e^- \rightarrow *CHOH$	0.59
$*CHOH + H^+ + e^- \rightarrow *CH + H_2O$	1.82
$*CH + H^+ + e^- \rightarrow *CH_2$	-1.46
$*CH_2 + H^+ + e^- \rightarrow *CH_3$	-1.70
$*CH_3 + H^+ + e^- \rightarrow *+CH_4$	-0.62
$*CO + H^+ + e^- \rightarrow *COH$	2.17
$*COH + H^+ + e^- \rightarrow *CHOH$	-1.17
$* + CO_2 + H^+ + e^- \rightarrow *HCOO$	0.23
$*HCOO + H^+ + e^- \rightarrow *HCOOH$	0.91
$*HCOOH + H^+ + e^- \rightarrow *CHO + H_2O$	-0.96

Table S10: Reaction steps and Gibbs free energy changes (ΔG, eV) of CO_2RR to CH_4 on Co-N-Ni at room temperature under 1 atm

Reaction steps	**ΔG (eV)**	
	Co site	Ni site
$* + CO_2 + H^+ + e^- \rightarrow *COOH$	0.27	1.10
$*COOH + H^+ + e^- \rightarrow *CO + H_2O$	-0.51	-0.25
$*CO + H^+ + e^- \rightarrow *CHO$	0.41	0.29
$*CHO + H^+ + e^- \rightarrow *OCH_2$	0.59	-0.16
$*OCH_2 + H^+ + e^- \rightarrow *OCH_3$	-0.19	0.36
$*OCH_3 + H^+ + e^- \rightarrow *O + CH_4$	0.36	1.19
$*O + H^+ + e^- \rightarrow *OH$	-1.32	-2.17
$*OH + H^+ + e^- \rightarrow * + H_2O$	-0.81	-1.56
$*CHO + H^+ + e^- \rightarrow *CHOH$	0.67	0.94
$*CHOH + H^+ + e^- \rightarrow *CH + H_2O$	1.79	1.93
$*CH + H^+ + e^- \rightarrow *CH_2$	-1.51	-1.87
$*CH_2 + H^+ + e^- \rightarrow *CH_3$	-1.69	-1.94
$*CH_3 + H^+ + e^- \rightarrow *+CH_4$	-0.62	-1.39
$*CO + H^+ + e^- \rightarrow *COH$	2.25	2.40
$*COH + H^+ + e^- \rightarrow *CHOH$	-1.16	-1.16
$* + CO_2 + H^+ + e^- \rightarrow *HCOO$	0.67	1.30
$*HCOO + H^+ + e^- \rightarrow *HCOOH$	-0.03	-1.20
$*HCOOH + H^+ + e^- \rightarrow *CHO + H_2O$	-0.47	1.04

Table S11: Reaction steps and Gibbs free energy changes (ΔG, eV) of CO_2RR to CH_4 on Co-N-Cu at room temperature under 1 atm

Reaction steps	**ΔG (eV)**	
	Co site	Cu site
$* + CO_2 + H^+ + e^- \rightarrow *COOH$	0.27	1.70
$*COOH + H^+ + e^- \rightarrow *CO + H_2O$	-0.36	-0.78
$*CO + H^+ + e^- \rightarrow *CHO$	0.10	0.65
$*CHO + H^+ + e^- \rightarrow *OCH_2$	0.76	-0.64
$*OCH_2 + H^+ + e^- \rightarrow *OCH_3$	-0.07	0.55
$*OCH_3 + H^+ + e^- \rightarrow *O + CH_4$	0.21	1.17
$*O + H^+ + e^- \rightarrow *OH$	-1.36	-2.15
$*OH + H^+ + e^- \rightarrow * + H_2O$	-0.74	-1.70
$*CHO + H^+ + e^- \rightarrow *CHOH$	0.91	0.67
$*CHOH + H^+ + e^- \rightarrow *CH + H_2O$	1.80	1.97
$*CH + H^+ + e^- \rightarrow *CH_2$	-1.53	-1.69
$*CH_2 + H^+ + e^- \rightarrow *CH_3$	-1.92	-1.93
$*CH_3 + H^+ + e^- \rightarrow *+CH_4$	-0.47	-1.77
$*CO + H^+ + e^- \rightarrow *COH$	2.19	2.86
$*COH + H^+ + e^- \rightarrow *CHOH$	-1.17	-1.54
$* + CO_2 + H^+ + e^- \rightarrow *HCOO$	0.48	1.28
$*HCOO + H^+ + e^- \rightarrow *HCOOH$	0.27	-0.84
$*HCOOH + H^+ + e^- \rightarrow *CHO + H_2O$	-0.74	1.14

Free energy diagrams of Co-N-M (M=Cr, Mn, Fe) at different applied potentials

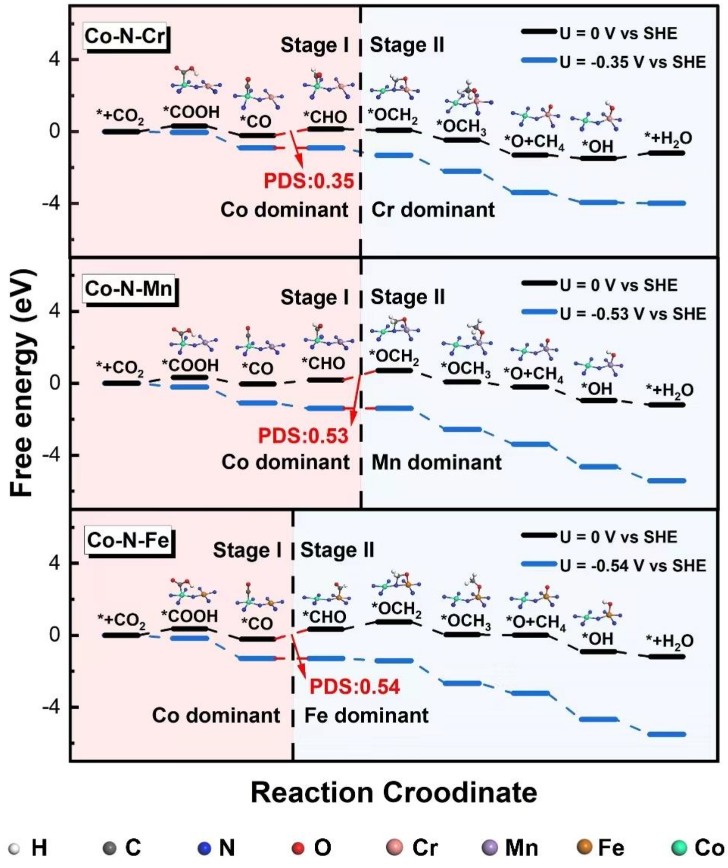

Fig. S17 Free energy diagrams of CO_2 reduction to CH_4 on Co sites (stage I, Co dominant), M sites (stage II, M dominant) of Co-N-M (M=Cr, Mn, Fe) in the inner tandem process with electrode potential U = 0 V, and corresponding U_L value.

Dynamic energy barriers of the first CO_2 hydrogenation step

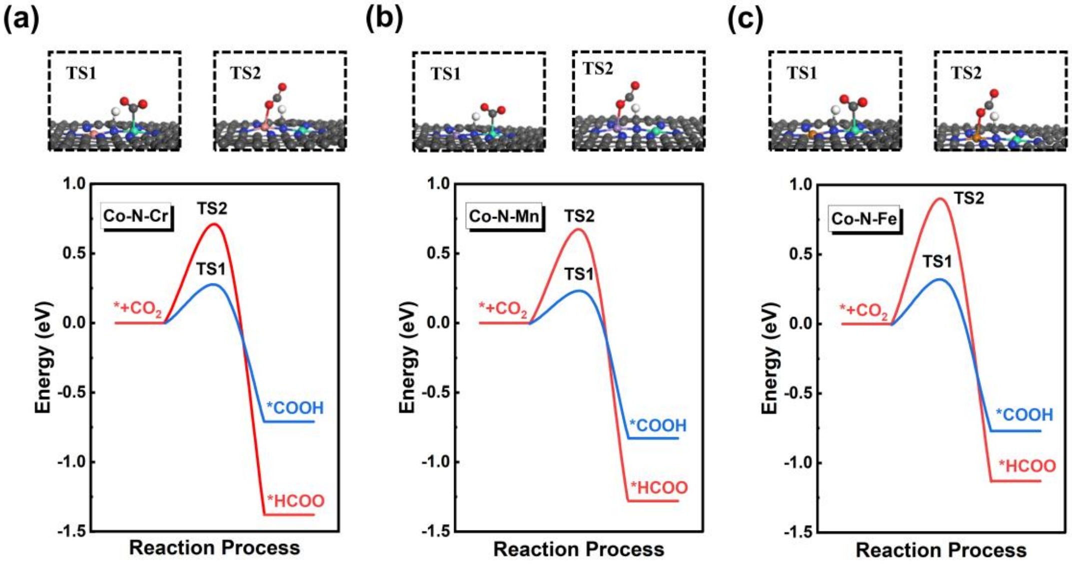

Fig. S18 The dynamic energy barriers of the first CO_2 hydrogenation step (*COOH or *HCOO formation) on (a) Co-N-Cr, (b) Co-N-Mn, and (c) Co-N-Fe.

Analysis of CO adsorption performance

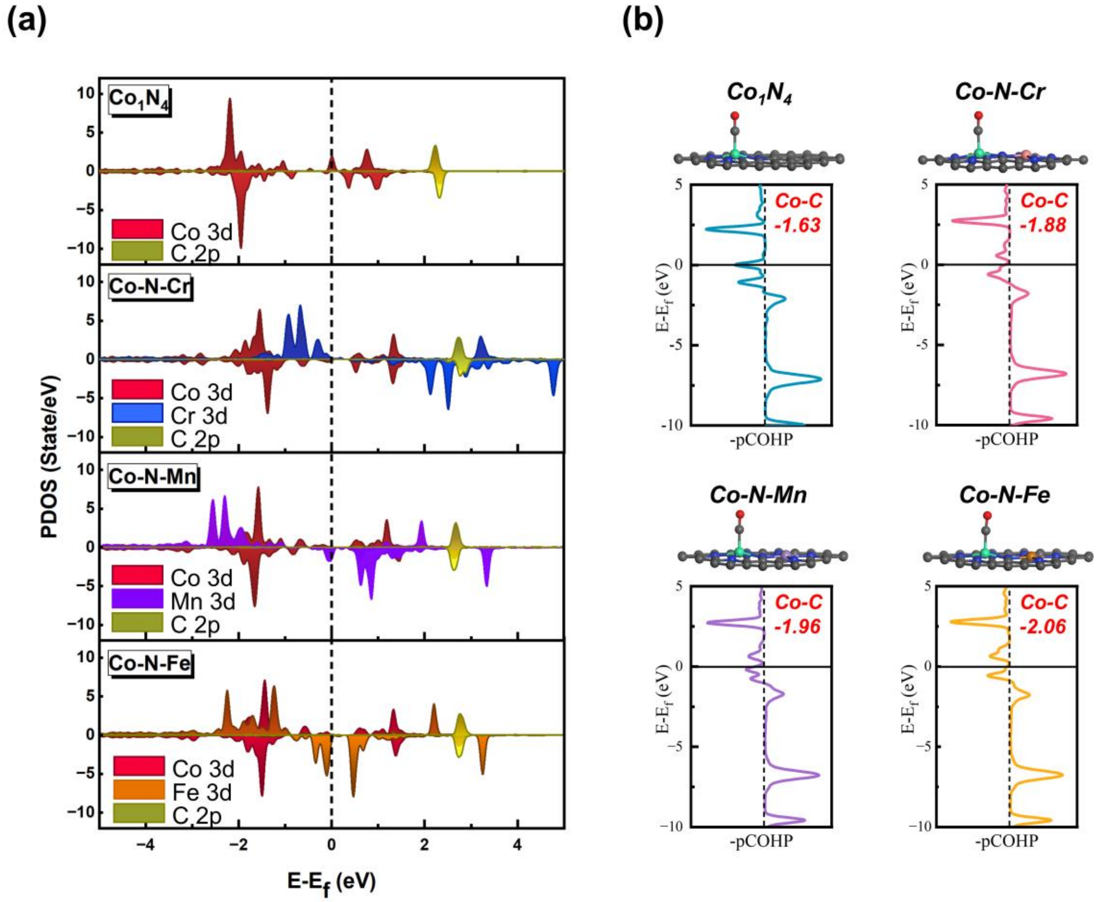

Fig. S19 (a) Calculated PDOS of the Co_1N_4 and Co-N-M (M=Cr, Mn, Fe), the dashed black line represents the Fermi level. (b) Projected crystal orbital Hamilton population (pCOHP) for the Co-C bonded of the Co_1N_4 and Co-N-M (M=Cr, Mn, Fe). The values of integrated COHP (ICOHP) are shown in red bold italics.

The linear scaling relationship between E_{ads} and the d-band center

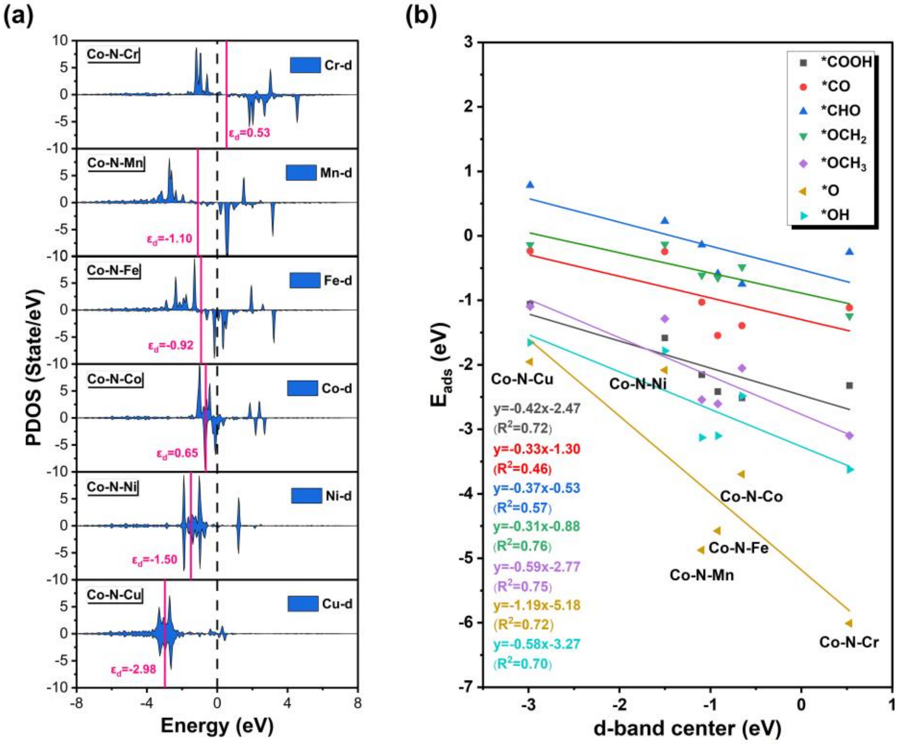

Fig. S20 (a) Projected density of states (PDOS) of d orbitals of the M atom on Co-N-M. The d-band center (εd) is marked by the purple line. The Fermi level is represented by the black dash line (set to zero). (b) The fitting linear relationships between E_{ads} of some important intermediates and the d-band center.

The stability and free energy diagrams of Co-N-M (M=Sc, Ti, V)

Table S12 The formation energy (E_f), standard dissolution potential (U^0_{diss}) and computed dissolution potential (U_{diss}) of metals, and the number of transferred electrons (n_e) of corresponding metal atom during the dissolution.

Catalysts	**E_f (eV)**	**U^0_{diss} (V)**		**U_{diss} (V)**	**n_e**
Co-N-Sc	-3.48	Co-N-Sc_Co	-0.28	0.75	2
		Co-N-Sc_Sc	-2.08	-0.44	3
Co-N-Ti	-2.82	Co-N-Ti_Co	-0.28	0.49	2
		Co-N-Ti_Ti	-1.63	-1.18	2
Co-N-V	-2.39	Co-N-V_Co	-0.28	0.50	2
		Co-N-V_V	-1.18	0.18	2

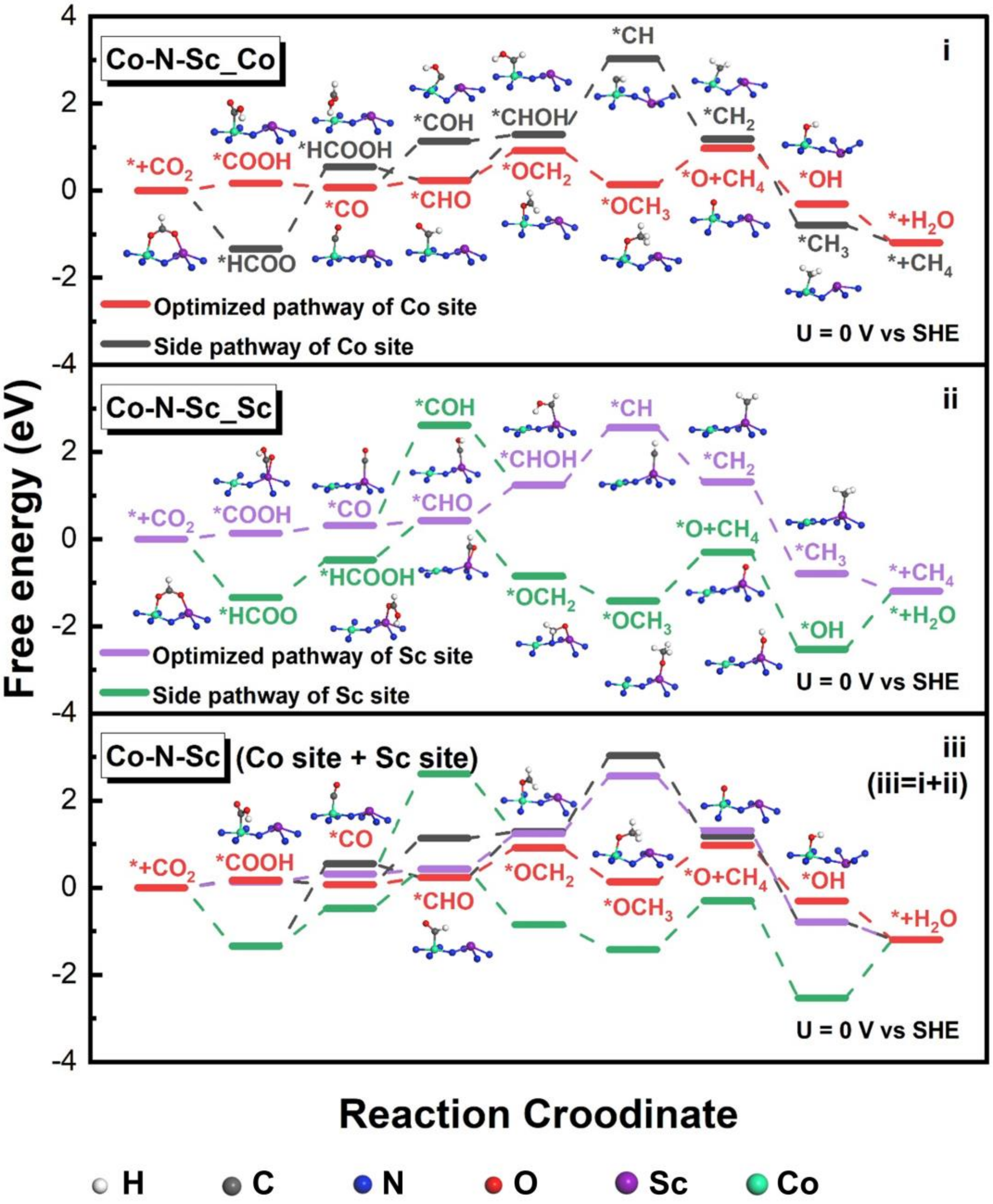

Fig. S21 Free energy diagrams and geometrical structures of CO_2 reduction to CH_4 on Co site (i), Sc site (ii) and the combinatorial pathway (iii) of Co-N-Sc.

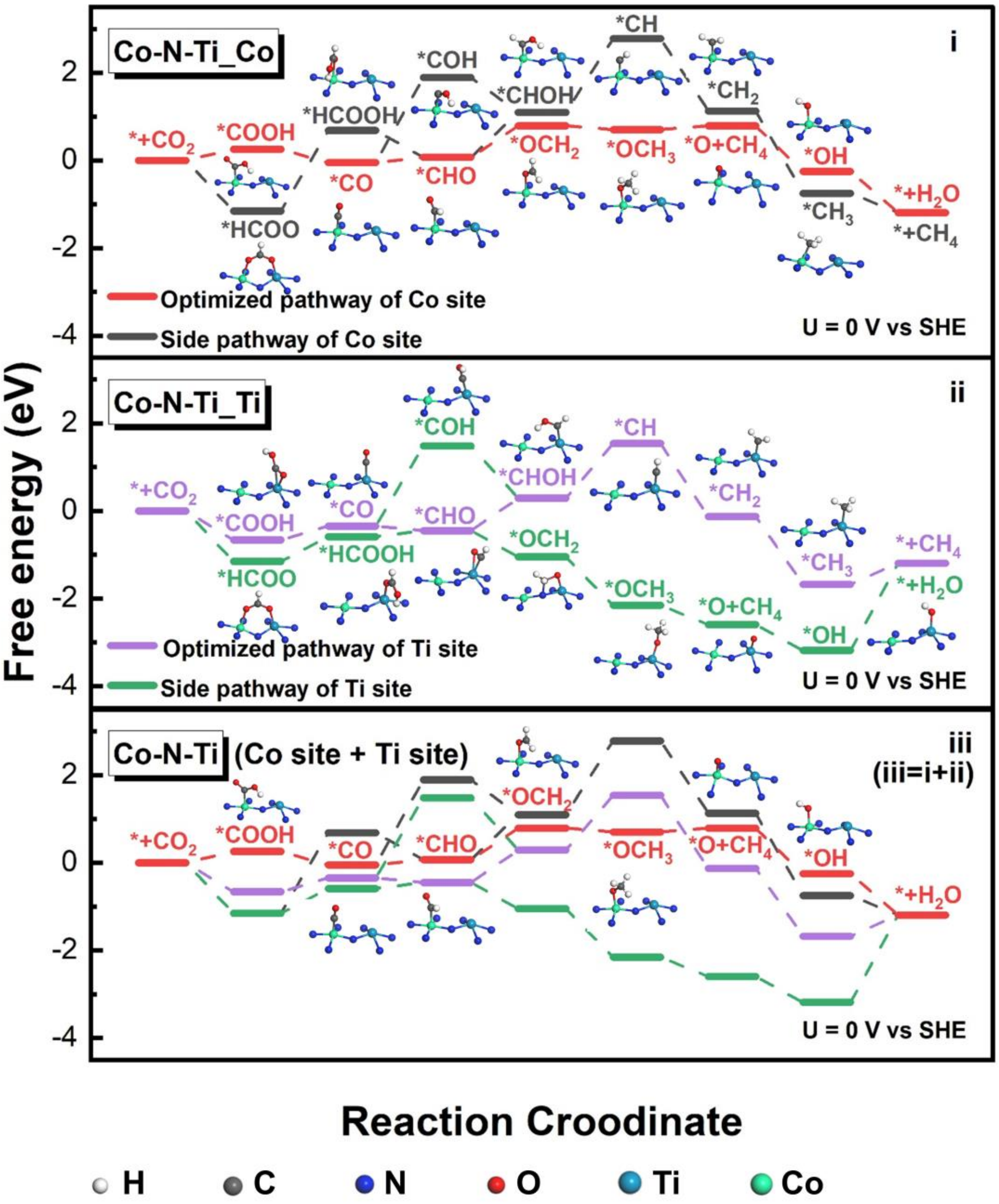

Fig. S22 Free energy diagrams and geometrical structures of CO_2 reduction to CH_4 on Co site (i), Ti site (ii) and the combinatorial pathway (iii) of Co-N-Ti.

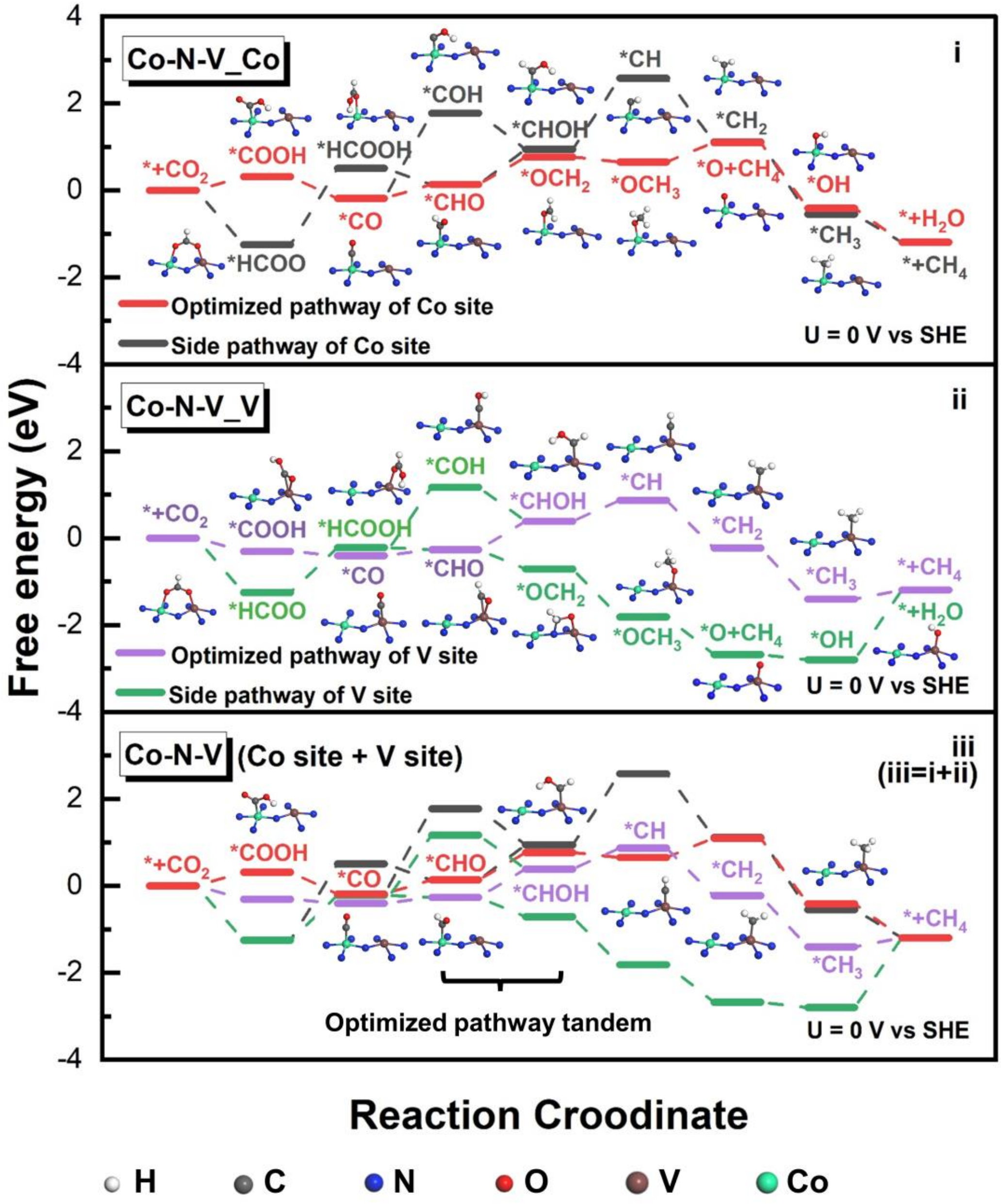

Fig. S23 Free energy diagrams and geometrical structures of CO_2 reduction to CH_4 on Co site (i), V site (ii) and the inner tandem combinatorial pathway (iii) of Co-N-V.

Reaction steps and ΔG of CO_2RR on Co-N-M (M=Sc, Ti, V)

Table S13: Reaction steps and Gibbs free energy changes (ΔG, eV) of CO_2RR to CH_4 on Co-N-Sc at room temperature under 1 atm.

Reaction steps	**ΔG (eV)**	
	Co site	Sc site
$* + CO_2 + H^+ + e^- \rightarrow *COOH$	0.17	0.14
$*COOH + H^+ + e^- \rightarrow *CO + H_2O$	-0.09	0.17
$*CO + H^+ + e^- \rightarrow *CHO$	0.16	0.12
$*CHO + H^+ + e^- \rightarrow *OCH_2$	0.69	-1.28
$*OCH_2 + H^+ + e^- \rightarrow *OCH_3$	-0.78	-0.57
$*OCH_3 + H^+ + e^- \rightarrow *O + CH_4$	0.83	1.12
$*O + H^+ + e^- \rightarrow *OH$	-1.28	-2.23
$*OH + H^+ + e^- \rightarrow * + H_2O$	-0.88	1.34
$*CHO + H^+ + e^- \rightarrow *CHOH$	1.06	0.81
$*CHOH + H^+ + e^- \rightarrow *CH + H_2O$	1.74	1.33
$*CH + H^+ + e^- \rightarrow *CH_2$	-1.85	-1.25
$*CH_2 + H^+ + e^- \rightarrow *CH_3$	-1.97	-2.10
$*CH_3 + H^+ + e^- \rightarrow *+CH_4$	-0.40	-0.40
$*CO + H^+ + e^- \rightarrow *COH$	1.06	2.30
$*COH + H^+ + e^- \rightarrow *CHOH$	0.16	-1.37
$* + CO_2 + H^+ + e^- \rightarrow *HCOO$	-1.34	-1.34
$*HCOO + H^+ + e^- \rightarrow *HCOOH$	1.88	0.86
$*HCOOH + H^+ + e^- \rightarrow *CHO + H_2O$	-0.31	0.90

Table S14: Reaction steps and Gibbs free energy changes (ΔG, eV) of CO_2RR to CH_4 on Co-N-Ti at room temperature under 1 atm.

Reaction steps	**ΔG (eV)**	
	Co site	Ti site
$* + CO_2 + H^+ + e^- \rightarrow *COOH$	0.26	-0.66
$*COOH + H^+ + e^- \rightarrow *CO + H_2O$	-0.31	0.32
$*CO + H^+ + e^- \rightarrow *CHO$	0.12	-0.10
$*CHO + H^+ + e^- \rightarrow *OCH_2$	0.72	-0.60
$*OCH_2 + H^+ + e^- \rightarrow *OCH_3$	-0.09	-1.10
$*OCH_3 + H^+ + e^- \rightarrow *O + CH_4$	0.09	-0.44
$*O + H^+ + e^- \rightarrow *OH$	-1.04	-0.59
$*OH + H^+ + e^- \rightarrow * + H_2O$	-0.94	2.00
$*CHO + H^+ + e^- \rightarrow *CHOH$	1.03	0.74
$*CHOH + H^+ + e^- \rightarrow *CH + H_2O$	1.69	1.25
$*CH + H^+ + e^- \rightarrow *CH_2$	-1.65	-1.66
$*CH_2 + H^+ + e^- \rightarrow *CH_3$	-1.88	-1.55
$*CH_3 + H^+ + e^- \rightarrow *+CH_4$	-0.44	0.49
$*CO + H^+ + e^- \rightarrow *COH$	1.94	1.83
$*COH + H^+ + e^- \rightarrow *CHOH$	-0.80	-1.20
$* + CO_2 + H^+ + e^- \rightarrow *HCOO$	-1.16	-1.16
$*HCOO + H^+ + e^- \rightarrow *HCOOH$	1.84	0.57
$*HCOOH + H^+ + e^- \rightarrow *CHO + H_2O$	-0.62	0.14

Table S15: Reaction steps and Gibbs free energy changes (ΔG, eV) of CO_2RR to CH_4 on Co-N-V at room temperature under 1 atm.

Reaction steps	**ΔG (eV)**		
	Co site	V site	Tandem site
$* + CO_2 + H^+ + e^- \rightarrow *COOH$	0.31	-0.30	0.31
$*COOH + H^+ + e^- \rightarrow *CO + H_2O$	-0.50	-0.10	-0.50
$*CO + H^+ + e^- \rightarrow *CHO$	0.32	0.14	0.32
$*CHO + H^+ + e^- \rightarrow *OCH_2$	0.63	-0.44	/
$*OCH_2 + H^+ + e^- \rightarrow *OCH_3$	-0.12	-1.10	/
$*OCH_3 + H^+ + e^- \rightarrow *O + CH_4$	0.44	-0.86	/
$*O + H^+ + e^- \rightarrow *OH$	-1.51	-0.13	/
$*OH + H^+ + e^- \rightarrow * + H_2O$	-0.77	1.61	/
$*CHO + H^+ + e^- \rightarrow *CHOH$	0.80	0.65	0.25
$*CHOH + H^+ + e^- \rightarrow *CH + H_2O$	1.64	0.48	0.48
$*CH + H^+ + e^- \rightarrow *CH_2$	-1.47	-1.10	-1.10
$*CH_2 + H^+ + e^- \rightarrow *CH_3$	-1.67	-1.17	-1.17
$*CH_3 + H^+ + e^- \rightarrow *+CH_4$	-0.64	0.21	0.21
$*CO + H^+ + e^- \rightarrow *COH$	1.96	1.57	/
$*COH + H^+ + e^- \rightarrow *CHOH$	-0.84	-0.78	/
$* + CO_2 + H^+ + e^- \rightarrow *HCOO$	-1.25	-1.25	/
$*HCOO + H^+ + e^- \rightarrow *HCOOH$	1.76	1.03	/
$*HCOOH + H^+ + e^- \rightarrow *CHO + H_2O$	-0.37	-0.05	/

The adsorption free energy of $C_xH_yO_z$

Table S16 The adsorption free energies ($\Delta G_{*CxHyOz}$, eV) of the intermediates with the C/O target on Co-N-M at room temperature under 1 atm

Co-N-M	Site	*COOH	*CO	*CHO	*OCH_2	*OCH_3	*O	*OH	*C	*CH_3
Co-N-Cr	Co	0.31	-0.21	0.14	0.76	0.63	2.10	0.80	3.05	-0.63
	Cr	0.44	0.08	0.68	0.08	-0.46	-0.11	-0.30	2.80	-0.66
Co-N-Mn	Co	0.32	-0.04	0.18	0.76	0.71	2.35	0.98	3.26	-0.56
	Mn	0.54	0.17	0.78	0.71	0.08	0.98	0.24	2.36	-0.52
Co-N-Fe	Co	0.37	-0.21	0.17	0.78	0.60	2.12	0.81	3.00	-0.56
	Fe	0.38	-0.33	0.33	0.75	0.03	1.20	0.29	1.83	-0.65
Co-N-Co	Co	0.27	-0.23	0.18	0.75	0.60	2.15	0.87	3.05	-0.57
Co-N-Ni	Co	0.27	-0.24	0.17	0.76	0.58	2.13	0.82	3.09	-0.57
	Ni	1.10	0.85	1.14	0.99	1.35	3.73	1.56	5.10	0.20
Co-N-Cu	Co	0.27	-0.09	0.01	0.78	0.70	2.10	0.74	3.13	-0.72
	Cu	1.70	0.92	1.57	0.93	1.48	3.85	1.70	5.75	0.58

The 3D plot of the scaling relationship

The 3D plots reduction to 2D method is as follows: firstly, the coefficients A and B are obtained by the function z = Ax + By + C in the 3D plots (z(x,y)), and then a new x is set to x = Ax + By to construct a new function of y = x + C for the 2D plots (y(x)).

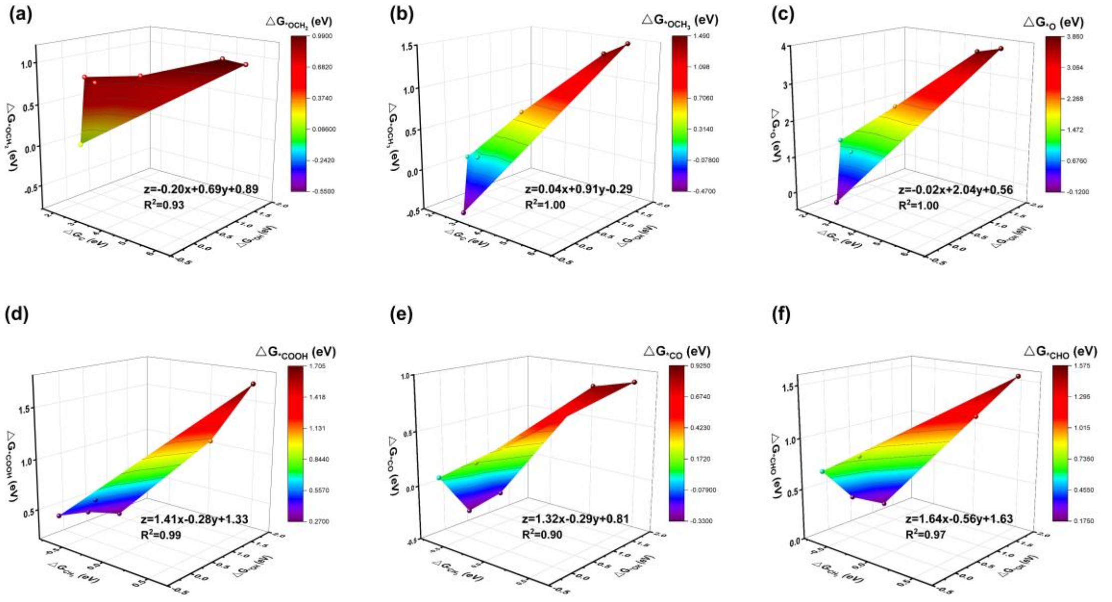

Fig. S24 The 3D plot of (a-c) the scaling relationships of the adsorption free energies of O-binding intermediates with combined descriptors of ΔG_{*C} and ΔG_{*OH}. The 3D plot of (d-f) the scaling relationships of the adsorption free energies of C-binding intermediates with combined descriptors of ΔG_{*CH_3} and ΔG_{*OH}. All ΔG were referenced to Gibbs free energies of CO_2(g), H_2(g), and H_2O(g).

References

[1] G. Kresse and J. Furthmuller, *Comput. Mater. Sci.*, 1996, **6**, 15-50.

[2] G. Kresse and J. Furthmuller, *Phys. Rev. B*, 1996, **54**, 11169-11186.

[3] J. P. Perdew, K. Burke and M. Ernzerhof, *Phys. Rev. Lett.*, 1996, **77**, 3865-3868.

[4] P. Blochl, *Phys. Rev. B*, 1994, **50**, 17953-17979.

[5] J. K. Norskov, J. Rossmeisl, A. Logadottir, L. Lindqvist, J. R. Kitchin, T. Bligaard and H. Jonsson, *J. Phys. Chem. B*, 2004, **108**, 17886-17892.

[6] Computational chemistry comparison and benchmark database. http://cccbdb.nist.gov/.

[7] L. Fu, R. Wang, C. Zhao, J. Huo, C. He, K.-H. Kim and W. Zhang, *Chem. Eng. J.*, 2021, **414**, 128857.

[8] J. Greeley and J. K. Nørskov, *Electrochim. Acta*, 2007, **52**, 5829-5836.

[9] X. Guo, J. Gu, S. Lin, S. Zhang, Z. Chen and S. Huang, *J. Am. Chem. Soc.*, 2020, **142**, 5709-5721.

[10] N. Shuichi, *Theor. Phys. Suppl.*, 1991, **103**, 1-46.

[11] H. Helmholtz, *Ann. Phys. Chem.*, 1879, **243**, 337-382.

[12] D. C. Grahame, *Chem. Rev*., 1947, **41**, 441-501.

[13] V. L. Deringer, A. L. Tchougréeff and R. Dronskowski, *J. Phys. Chem. A*, 2011, **115**, 5461-5466.

[14] R. Dronskowski and P. E. Bloechl, *J. Phys. Chem.*, 1993, **97**, 8617-8624.

[15] S. Maintz, V. L. Deringer, A. L. Tchougréeff and R. Dronskowski, *J. Comput. Chem.*, 2016, **37**, 1030-1035.

[16] G. Henkelman and H. Jónsson, *J. Chem. Phys.*, **2000**, *113*, 9978-9985.

[17] G. Henkelman, B. P. Uberuaga and H. Jónsson, *J. Chem. Phys.*, 2000, **113**, 9901-9904.